Influence of varied doping structure on photoemissive property of photocathode*

Niu Jun(牛 军)[a)b)], Zhang Yi-Jun(张益军)[a)],
Chang Ben-Kang(常本康)[a)†], and Xiong Ya-Juan(熊雅娟)[a)]

[a)] *School of Electronic Engineering and Optoelectronic Technology, Nanjing University of Science and Technology, Nanjing* 210094, *China*

[b)] *Department of Electron and Electric Engineering, Nanyang Institute of Technology, Nanyang* 473004, *China*

(Received 10 August 2010; revised manuscript received 14 December 2010)

The built-in electric fields within a varied doping GaAs photocathode may promote the transport of electrons from the bulk to the surface, thus the quantum efficiency of the cathode can be enhanced remarkably. But this enhancement, which might be due to the increase in either the number or the energy of electrons reaching the surface, is not clear at present. In this paper, the energy distributions of electrons in a varied doping photocathode and uniform doping photocathode before and after escaping from the cathode surface are analysed, and the number of electrons escaping from the surface in different cases is calculated for the two kinds of photocathodes. The results indicate that the varied doping structure can not only increase the number of electrons reaching the surface but also cause an offset of the electron energy distribution to high energy. That is the root reason for the enhancement of the quantum efficiency of a varied doping GaAs photocathode.

Keywords: varied doping, photocathode, energy distribution, quantum efficiency

PACS: 42.70.Gi, 42.79.Pw, 71.55.Eq, 72.10.Bg **DOI:** 10.1088/1674-1056/20/4/044209

1. Introduction

Transmission-mode negative electron affinity (NEA) GaAs photocathodes have found an important use as the core component of the third-generation low light level (LLL) image intensifier. Its photoemissive property is determined not only by the activation technique for NEA photocathodes but also by the cathode material's own growth level. In recent years, in order to enhance the quantum efficiency of the NEA GaAs photocathode, varied doping cathode material has been proposed and become the research hotspot.[1−6] Within the varied doping GaAs photocathode material, a built-in electric field directed from the GaAs bulk to the surface can be formed, which can affect the transport of photoelectrons towards the cathode surface. One possible result of the effects of the built-in electric field is that the number of photoelectrons reaching the cathode surface is increased, while another possible result is that the whole energy of the photoelectrons reaching the surface is enhanced. Thus the electron escape probability is improved. Any of the two results may be responsible for the enhancement of the quantum efficiency of a varied doping GaAs photocathode, but the real result of the varied doping structure is still not fully understood at present. In this paper, based on experimental results, the influence of the varied doping structure on the cathode photoemissive property is investigated and analysed according to the energy distributions of electrons before and after escaping from the cathode surface.

2. Experiment

Two kinds of transmission-mode GaAs photocathode materials were grown by the molecular beam epitaxy (MBE) technique. The 1.6-μm thick active layers in both samples were p-type Be heavily doped. Of them, sample 1 is uniformly doped with a doping concentration of 1×10^{19} cm^{-3}, and sample 2 is varied doped with doping concentrations in a range of 1×10^{19} cm^{-3}–1×10^{18} cm^{-3} from the bulk to the surface.

The cathode samples were cleaned by a general

*Project supported by the National Natural Science Foundation of China (Grant No. 60678043) and the Research and Innovation Plan for Graduate Students of Jiangsu Higher Education Institutions of China (Grant No. CX09B_096Z).

†Corresponding author. E-mail: bkchang@mail.njust.edu.cn

© 2011 Chinese Physical Society and IOP Publishing Ltd

technique and made into the cathode modules with a glass/Si_3N_4/GaAlAs/GaAs structure. Then the samples were activated in an ultrahigh vacuum chamber by using the "high-low temperature tow-step" activation technique. In the activation process, a cesium source was kept continuously and an oxygen source was opened and closed periodically. Before the experiment, the system vacuum level was above 1×10^{-8} Pa, and in the heat cleaning process it was above 2×10^{-8} Pa. When the sample temperature was cooled down to 60 °C after heat cleaning, the activation began and the vacuum level returned to 1×10^{-8} Pa.

After activation, the cathode modules were sealed into the third-generation image intensifier tubes, in which the microchannel plate (MCP) and fluorescence screen were removed. Then the spectral responses of the sealed image tubes were measured by the spectral response measurement instrument. The spectral response curves ranging from 600 nm to 1000 nm for both samples are shown in Fig. 1. The measured integral sensitivities of the two samples are 1150 μA/lm and 1572.5 μA/lm, respectively, and thus the integral sensitivity of a varied doped photocathode is 1.36 times that of a uniform doped photocathode.

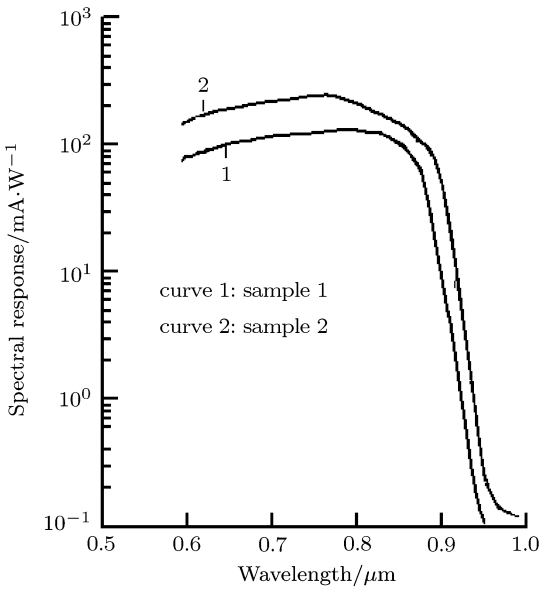


Fig. 1. Spectral response curves of the two cathode samples.

3. Simulation and calculation

From the comparison between curves in Fig. 1, it follows that the varied doping structure applied to the activation layer can increase the spectral response sensitivity by more than 30%. The increase in spectral response sensitivity corresponds to the increase in the number of electrons tunneling through the surface potential barrier and entering into the vacuum. In order to discover the root cause of the increase in electron number, it is necessary to analyse the electron energy distribution.

For the transmission-mode photocathode, the energetic electrons are excited mainly in the region near the back-interface. When they pass through a long distance and reach the surface band bending region, most of them have been thermalized at the bottom of the Γ conduction band minimum. Their energy distribution at this point is determined by the room-temperature Maxwell–Boltzmann distribution in the form[7,8]

$$n_d(\Delta E) \propto \Delta E^{1/2} \cdot \exp(-\Delta E/kT), \tag{1}$$

where k is the Boltzmann's constant, T is the absolute temperature, and ΔE is the kinetic energy of the electron in the conduction band minimum. The electron energy distribution curve is shown in Fig. 2(a). The width d of the surface band bending region can be calculated by[7]

$$d = \left(\frac{2\delta_s\varepsilon_0\varepsilon}{n_A e}\right)^{1/2}, \tag{2}$$

where n_A is the surface-layer doping concentration, e is the electronic charge, δ_s is the amount of band bending, and ε_0 and ε are the vacuum dielectric constant and the relative dielectric constant of GaAs, respectively. From Fig. 2, we know that the concentration significantly affects the width of the band bending region. Because the surface-layer doping concentration of the varied doped cathode sample is 1×10^{18} cm^{-3}, which is less than that of the uniform doped cathode sample, the width d of sample 2 will be larger than that of sample 1, which is disadvantageous to the cathode photoemission.

Electrons entering the space-charge region are accelerated by the internal electric field towards the surface. Meanwhile, they suffer hot-electron–phonon interactions. The energy distribution of electrons reaching the surface is obtained from a solution of the Boltzmann transport equation. According to the calculations in Refs. [9] and [10], we obtain the energy distribution curves of electrons reaching the surface for the two samples, which are shown in Fig. 2(b), where curves 1 and 2 are normalized and correspond to samples 1 and 2, respectively.

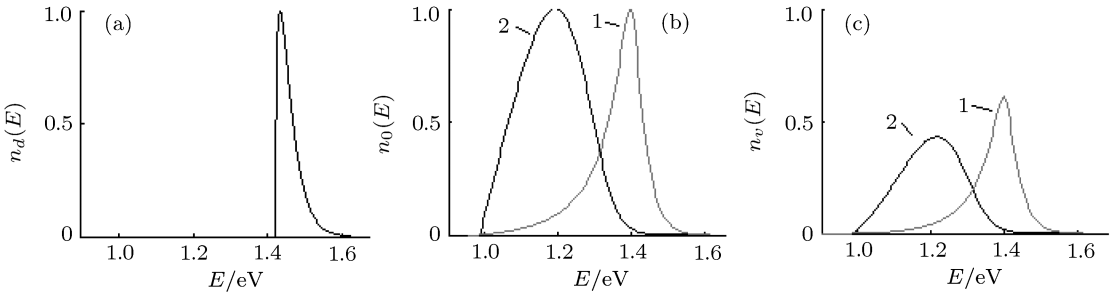


Fig. 2. Electron energy distributions.

The profile of the surface barrier comprises two approximately straight lines with different slopes, as shown in Fig. 3, which are called barriers I and II.

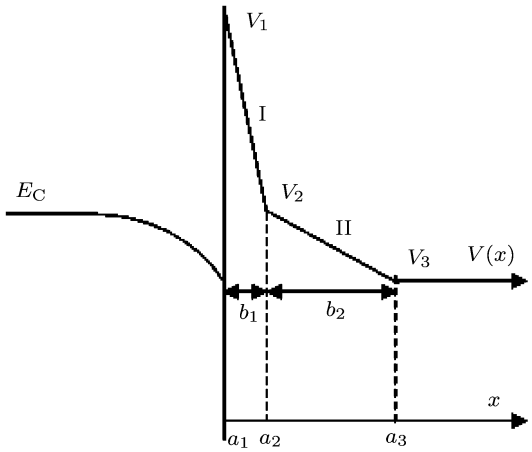


Fig. 3. Illustration of double dipole surface model.

This profile is proposed based on the double-dipole model.[11,12] Barriers I and II are created by dipoles I and II, respectively. Accordingly, the surface potential function is

$$V(x) = -F_i(x - b_i), \tag{3}$$

where $i = 1, 2$, $a_i < x < a_{i+1}$, $b_i = a_i + V_i/F_i$, and $F_i = -(V_{i+1} - V_i)/(a_{i+1} - a_i)$.

The one-dimensional time-independent Schrödinger wave equation in barriers I and II is given by

$$\frac{\mathrm{d}^2\psi(x)}{\mathrm{d}^2x} - \frac{2m}{\hbar^2}\left[V(x) - E\right]\psi(x) = 0. \tag{4}$$

Because $V(x)$ is a piecewise-linear potential function, the solution of the Schrödinger equation across the interval $(a_i,\ a_{i+1})$ can be expressed in a linear combination of the Airy functions as[13–15]

$$\psi_i(x) = C_i^+\mathrm{Ai}(z_i) + C_i^-\mathrm{Bi}(z_i), \tag{5}$$

where $z_i = r_i(x - c_i)$, $r_i = -(2mF_i/\hbar^2)^{1/3}$, $c_i = a_i + (V_i - E)/F_i$, Ai and Bi are the Airy functions, C_i^+ and C_i^- are the coefficients to be determined, m is the electron effective mass, E is the incident electron energy, and h is the reduced Planck constant.

According to the boundary conditions at the interface a_{i+1} that are met by the wave function, and the wave function in the regions $x < a_1$ and $x > a_3$, the following equation can be obtained,

$$\begin{aligned}
\begin{bmatrix} C_0^+ \\ C_0^- \end{bmatrix} &= \frac{1}{2}\begin{bmatrix} 1 & -\frac{\mathrm{i}}{k_0} \\ 1 & \frac{\mathrm{i}}{k_0} \end{bmatrix}\begin{bmatrix} \mathrm{Ai}(r_1(a_1 - c_1)) & \mathrm{Bi}(r_1(a_1 - c_1)) \\ r_1\mathrm{Ai}'(r_1(a_1 - c_1)) & r_1\mathrm{Bi}'(r_1(a_1 - c_1)) \end{bmatrix} \\
&\times \begin{bmatrix} \mathrm{Ai}(r_1(a_2 - c_1)) & \mathrm{Bi}(r_1(a_2 - c_1)) \\ r_1\mathrm{Ai}'(r_1(a_2 - c_1)) & r_1\mathrm{Bi}'(r_1(a_2 - c_1)) \end{bmatrix}^{-1}\begin{bmatrix} \mathrm{Ai}(r_2(a_2 - c_2)) & \mathrm{Bi}(r_2(a_2 - c_2)) \\ r_2\mathrm{Ai}'(r_2(a_2 - c_2)) & r_2\mathrm{Bi}'(r_2(a_2 - c_2)) \end{bmatrix} \\
&\times \begin{bmatrix} \mathrm{Ai}(r_2(a_3 - c_2)) & \mathrm{Bi}(r_2(a_3 - c_2)) \\ r_2\mathrm{Ai}'(r_2(a_3 - c_2)) & r_2\mathrm{Bi}'(r_2(a_3 - c_2)) \end{bmatrix}^{-1}\begin{bmatrix} 1 & 1 \\ \mathrm{i}\,k_3 & -\mathrm{i}\,k_3 \end{bmatrix}\begin{bmatrix} C_3^+ \\ C_3^- \end{bmatrix} \\
&= \begin{bmatrix} M_{11} & M_{12} \\ M_{21} & M_{22} \end{bmatrix}\begin{bmatrix} C_3^+ \\ C_3^- \end{bmatrix},
\end{aligned} \tag{6}$$

where $r_1 = -(2mF_1/\hbar^2)^{1/3}$, $c_1 = a_1 + (V_1 - E)/F_1$, $r_2 = -(2mF_2/\hbar^2)^{1/3}$, and $c_2 = a_2 + (V_2 - E)/F_2$ with $F_1 = -(V_2 - V_1)/b_1$ and $F_2 = -(V_3 - V_2)/b_2$.

Since there is no reflection in the vacuum, the coefficient C_3^- is zero, then the transmission coefficient T is given as[15]

$$T = \frac{k_3}{k_0}\left|\frac{1}{M_{11}}\right|^2, \tag{7}$$

where $k_0 = \sqrt{2mE}/\hbar$, $k_3 = \sqrt{2m(E - V_3)}/\hbar$, and M_{11} is the value of the row 1/colum 1 element of the transfer matrix M. In Eq. (7), the transmission coefficient T is a function of the incident electron energy, the height and the width of the barrier.

Using Eq. (7), the energy distribution of electrons tunneling through the surface barrier can be obtained, and the results are shown in Fig. 2(c). In the calculations, we have assumed the widths to be 0.5 Å and 6 Å (1 Å=0.1 nm), and the heights to be 1.42 eV and 0.9 eV of barriers I and II, respectively.

The total number of electrons can be solved by calculating the integral of the electron energy distribution function. Therefore, utilizing the curves in Figs. 2(b) and 2(c), we can carry out relevant theoretical analysis of the change in the number of electrons before and after escaping from the cathode surface. First, we make the following assumptions:

a) The number of electrons remains unchanged before and after escaping.

b) The structures of surface potential barriers of the two cathode samples are the same, because their activation technique and experimental condition are exactly the same.

c) The total number of electrons escaping from the surface in the varied doping cathode is 1.3–1.4 times that in the uniform doping cathode.

For the varied doping cathode, the number of escaped electrons can be increased in the following three cases:

i) Because the varied doping structure is conducive to improvement of the electron diffusion and drift length, the number of electrons capable of reaching the surface is greatly increased, but the energy distribution remains unchanged.

ii) Electrons reaching the surface do not increase in number, but their energy is enhanced due to the action of the built-in electric field, and thus their surface transmission coefficient increases.

iii) Both the number and the energy of the electrons reaching the surface are increased.

Next, analysis and calculation are carried out in the above three cases. respectively.

In the first case, we assume that for samples 1 and 2, the energy distributions of electrons arriving at the band bending region conform to Eq. (1). Meanwhile, the electron number of sample 2 is larger than that of sample 1 because the electron diffusion and drift length of the varied doping cathode is larger than the electron diffusion length of the uniform doping cathode. On the assumption that the number of electrons escaping from the surface in the varied doped cathode is 1.3–1.4 times that in the uniform doped cathode, we can calculate the number of electrons before and after escaping the surface for the two samples according to the electron energy distribution curves shown in Fig. 2. The calculated results are listed in Table 1, where n_1 and n_2 are the calculated electron numbers of samples 1 and 2, respectively, which are not the actual electron numbers of the samples but the relative and theoretical values.

Table 1. Electron numbers before and after escaping from the surface.

	n_1 (sample 1)	n_2 (sample 2)	n_2/n_1
before escaping	22.7	52.1	2.30
after escaping	5.9	7.8	1.32

In the second case, we assume that when electrons arrive at the surface band bending region, due to the action of the built-in electric field in the electron transport process from the bulk to the surface, the energy of the electrons in the varied doping cathode is higher than that in the uniform doping cathode. Previous investigation indicates that in the varied doping cathode, if the doping concentration of the innermost layer is one order of magnitude higher than that of the surface layer, the electron energy increases by about 0.06 eV.[2] For the electron energy distribution expressed by Eq. (1), it is indicated from Fig. 2(a) that the electrons are mainly concentrated in the range from the conduction band minimum to 0.2 eV above the minimum. Therefore, assuming that the electron energy lost in the transport process towards the surface in the varied doping cathode is the same as that in the uniform doping cathode, then for sample 2 the electrons reaching the surface should be mainly concentrated in the range from the conduction band minimum to 0.26 eV above the minimum. The electron energy distribution for sample 2 is revised based on Eq. (1) and is expressed as

$$n_d(\Delta E) \propto \Delta E^2 \cdot \exp\left(-\Delta E/kT\right). \tag{8}$$

The electron energy distribution curve according to Eq. (8) is shown as curve 2 in Fig. 4(a), where curve

1 is for sample 1. From curve 2, we know that the energies of electrons are mainly concentrated in the range from the conduction band minimum to 0.26 eV above the minimum. Therefore, in order to carry out the analysis conveniently, we assume that the energy distribution of electrons arriving at the surface band bending region for sample 2 conforms to Eq. (8). At this point, the energy distribution curves for electrons before and after escaping from the surface are obtained and shown in Figs. 4(b) and 4(c), where curves 1 and 2 correspond to samples 1 and 2, respectively. In Fig. 4(b), in order to embody the same number of electrons in samples 1 and 2, the curves are not normalized, as shown in Fig. 2(b). The calculated number of electrons is shown in Table 2. In calculation, we have assumed that the number of electrons before escaping from the surface in samples 1 and 2 is the same.

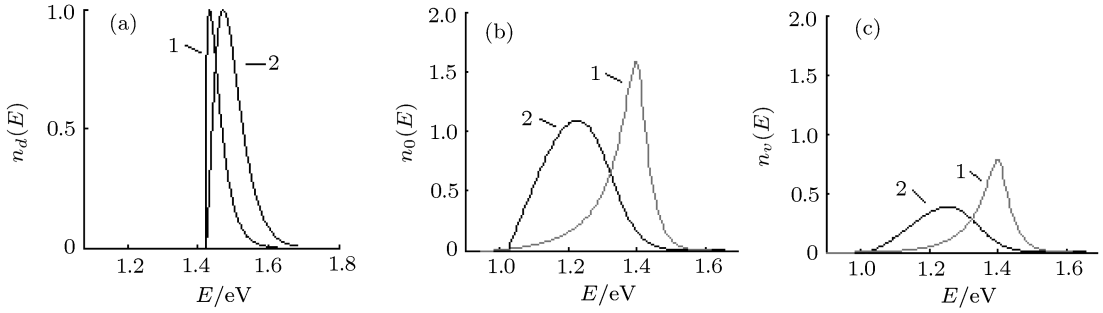


Fig. 4. Electron energy distributions for samples 1 and 2.

Table 2. Electron numbers before and after escaping from the surface.

	n_1 (sample 1)	n_2 (sample 2)	n_2/n_1
before escaping	51.1	51.3	1.0
after escaping	23.5	20.9	0.89

In the third case, we assume that for sample 2, the energy distribution of electrons arriving at the surface band bending region conforms to Eq. (8). Meanwhile, the total number of electrons reaching the surface is larger than that of sample 1. According to the principle that the number of electrons escaping from the surface will be increased by 30%–40% for the varied doping cathode, we calculate the numbers of electrons in samples 1 and 2, and the results are listed in Table 3.

Table 3. Electron numbers before and after escaping from the surface.

	n_1 (sample 1)	n_2 (sample 2)	n_2/n_1
before escaping	51.1	77.0	1.51
after escaping	23.5	31.3	1.33

4. Discussion

The calculated results in the above three cases are discussed as follows.

(i) From the first case, we know that if the electron energy distribution in the varied doping cathode does not change, then in order to meet the condition that the number of escaped electrons in sample 2 is 32% higher than that in sample 1, the number of electrons reaching the surface in sample 2 must be 2.3 times that in sample 1. But this is impossible to achieve, so this case is not likely to occur.

(ii) For the second case, limited by the doping structure, the most increased energy for electrons in sample 2 is only 0.06 eV.[2] In addition, the closer to the surface the electron is excited, the less the energy is increased. If the electrons reaching the surface are not increased in number, then the number of electrons escaping from the surface is only 0.89 times that in sample 1, which disaccords with the experimental result. Therefore, this case is not likely to occur either.

(iii) For the third case, in sample 2, due to the action of the built-in electric field, the energies of electrons are increased universally during the transport process from the bulk to the surface. The most increased energy we assumed is about 0.06 eV, which is in reasonable accordance with the actual potential difference formed by the doping structure. In addition, because the electron diffusion and drift length are increased,[3] the number of electrons that are able to reach the surface is increased correspondingly. If the total number of escaped electrons of sample 2 is increased by 33% over that of sample 1, the electrons reaching the surface should be 1.51 times that in sam-

ple 1, which is relatively reasonable. Therefore, this case is considered to be consistent with fact.

Based on the above analyses, we can draw the following conclusion: for the varied doping cathode, due to the effect of the built-in electric field, the number of electrons reaching the surface is increased, and an offset of the electrons energy distribution to high energy is incurred as well. As a result, the quantum efficiency of the varied doping cathode will be increased considerably.

In order to make it clear which cause is more important, further study should be carried out. In the third case, with the change in electron energy distribution unconsidered and the number of electrons reaching the surface in sample 2 assumed to be 1.51 times that in sample 1, the ratio of the escaped electrons of sample 2 to that of sample 1 is calculated to be 1.24, which indicates that in the third case, the improved cathode quantum efficiency caused by the increased electrons reaching the surface accounts for 72% of the total improvement. Therefore, compared with the change in the electron energy distribution, the drift electric field increased the number of electrons reaching the cathode surface makes a greater contribution to the enhancement of the cathode quantum efficiency.

5. Conclusion

The experimental results indicate that the quantum efficiency of the varied doping cathode can be increased by 30% over that of the uniform doping cathode. In order to clearly understand how the varied doping structure affects the photoemissive properties of the cathode concretely, the electron energy distribution of the transmission-mode photocathode is analysed. By simulation, the number of electrons before and after escaping from the surface are calculated in three cases, respectively. It is concluded that the varied doping structure can not only increase the number of photoelectrons reaching the surface but also cause an offset of the electron energy distribution to high energy. That is the root reason for the enhancement of quantum efficiency. The result of this paper is significant for the understanding of the photoemission process of varied doping GaAs photocathodes.

References

[1] Zou J J, Chang B K, Yang Z, Zhang Y J and Qiao J L 2009 *Acta Phys. Sin.* **58** 5842 (in Chinese)

[2] Zou J J, Chang B K and Yang Z 2009 *Acta Phys. Sin.* **58** 2992 (in Chinese)

[3] Niu J, Zhang Y J, Chang B K, Yang Z and Xiong Y J 2009 *Appl. Opt.* **48** 5445

[4] Niu J, Yang Z, Chang B K, Qiao J L and Zhang Y J 2009 *Acta Phys. Sin.* **58** 5002 (in Chinese)

[5] Zhang Y J, Chang B K, Yang Z, Niu J, Xiong Y J, Shi F, Guo H and Zeng Y P 2009 *Appl. Opt.* **48** 1715

[6] Zhang Y J, Chang B K, Yang Z, Niu J and Zou J J 2009 *Chin. Phys.* B **18** 4541

[7] Fisher D G, Enstrom R E, Escher J S and Williams B F 1972 *J. Appl. Phys.* **43** 3815

[8] Vergara G, Herrera-Gómez A and Spicer W E 1999 *Surf. Sci.* **436** 83

[9] Bartelink D J, Moll J L and Meyer N L 1963 *Phys. Rev.* **130** 972

[10] Williams B F and Simon R E 1967 *Phys. Rev. Lett.* **18** 485

[11] Su C Y, Chye P W, Pianetta P, Lindau I and Spicer W E 1979 *Surf. Sci.* **86** 894

[12] Su C Y, Lindau I and Spicer W E 1982 *Chem. Phys. Lett.* **87** 523

[13] Wang H M and Zhang Y F 2005 *Acta Phys. Sin* **54** 2226 (in Chinese)

[14] Lui W W and M Fukuma 1986 *J. Appl. Phys.* **60** 1555

[15] Zou J J, Chang B K, Yang Z, Zhang Y J and Qiao J L 2009 *J. Appl. Phys.* **105** 013714